



# Puzzles in eta photoproduction: the 1685 MeV narrow peak<sup>\*</sup>

B. Golli<sup>a,c</sup> and S. Širca<sup>b,c</sup>

<sup>a</sup> Faculty of Education, University of Ljubljana, 1000 Ljubljana, Slovenia

<sup>b</sup> Faculty of Mathematics and Physics, University of Ljubljana, 1000 Ljubljana, Slovenia

<sup>c</sup> and Jožef Stefan Institute, 1000 Ljubljana, Slovenia

**Abstract.** We claim that a narrow peak in the cross section near 1685 MeV in the  $\gamma n \rightarrow \eta n$  channel can be explained through a peculiar radial behaviour of the p-wave quark states with  $j = 1/2$  and  $j = 3/2$  in the low lying S11 resonances and the opening of the  $K\Sigma$  threshold rather than by an exotic resonance. We explain the mechanism of its formation in the framework of a coupled channel formalism which incorporates quasi-bound quark-model states corresponding to the two low lying resonances in the S11 partial wave. A relation to the Single Quark Transition Model is pointed out.

## 1 Motivation

In this contribution we discuss a possible quark-model explanation for a narrow structure at  $W \approx 1685$  MeV in the  $\gamma n \rightarrow \eta n$  reaction observed by the GRAAL Collaboration [1] which, however, turned out to be absent in the  $\eta p$  channel. Azimov *et al.* [2] were the first to discuss the possibility that the structure could belong to a partner of the  $\Theta^+$  pentaquark in the exotic antidecuplet of baryons. More conventional explanations have attributed the peak to the threshold effect of the  $K\Sigma$  channel [3], interference of the nearby  $S_{11}$ ,  $P_{11}$  and  $P_{13}$  resonances [4], constructive and destructive interference of the two lowest  $S_{11}$  resonances in the  $\eta n$  and  $\eta p$  channels, respectively, as anticipated in the framework of the Giessen model [5,6] as well as in the Bonn-Gatchina analysis [7,8]. In the framework of the constituent-quark model coupled to the pseudoscalar meson octet the (non)appearance of the peak was related to different EM multipoles (at the quark level) responsible for excitation in either of the two channels [9].

## 2 The coupled channel approach

In our recent paper [10] we have systematically analysed the partial waves with sizable contributions to the  $\eta N$ ,  $K\Lambda$  and  $K\Sigma$  decay channels using a SU(3) extended version of the Cloudy Bag Model (CBM) [11] which includes also the  $\rho$  and  $\omega$  mesons<sup>1</sup>. We have found that the main contribution to  $\eta$  photoproduction

<sup>\*</sup> Talk delivered by B. Golli

<sup>1</sup> The method has been described in detail in our previous papers [12–16] where we have analysed the scattering and electro-production amplitudes in different partial waves.

at low and intermediate energies comes from the S11 partial wave. In this contribution we therefore concentrate on the S11 partial wave in which the considered phenomenon is most clearly visible.

In our approach the main contribution to  $\eta$  production in the S11 partial wave stems from the resonant part of the electroproduction amplitude which can be cast in the form

$$\mathcal{M}_{\eta N \gamma N}^{\text{res}} = \sqrt{\frac{\omega_\gamma E_N^\gamma}{\omega_\pi E_N}} \frac{\xi}{\pi \mathcal{V}_{N\mathcal{R}}^\pi} \langle \Psi_{\mathcal{R}} | V_\gamma | \Psi_N \rangle T_{\eta N \pi N}, \quad (1)$$

where  $T_{\eta N \pi N}$  is the T-matrix element pertinent to the  $\pi N \rightarrow \eta N$  channel,  $V_\gamma$  describes the interaction of the photon with the electromagnetic current and  $\xi$  is the spin-isospin factor depending on the considered multipole and the spin and isospin of the outgoing hadrons. Here  $|\Psi_{\mathcal{R}}\rangle = c_1(W)|N(1535)\rangle + c_2(W)|N(1650)\rangle$  with

$$\begin{aligned} |N(1535)\rangle &= \cos \vartheta |70, 28, J = \frac{1}{2}\rangle - \sin \vartheta |70, 48, J = \frac{1}{2}\rangle, \\ |N(1650)\rangle &= \sin \vartheta |70, 28, J = \frac{1}{2}\rangle + \cos \vartheta |70, 48, J = \frac{1}{2}\rangle \end{aligned}$$

and  $c_i(W)$  are  $W$ -dependent coefficients determined in the coupled-channel calculation for scattering.

The strong  $T_{\eta N \pi N}$  amplitude is obtained in a coupled channel calculation with ten channels involving  $\pi$ ,  $\rho$ ,  $\omega$ ,  $\eta$  and  $K$  mesons. The most important channels are shown in Fig. 1. The behaviour of the amplitudes is dominated by the  $N(1535)$  and  $N(1650)$  resonances as well as the  $\eta N$ ,  $K\Lambda$  and  $K\Sigma$  thresholds. In the

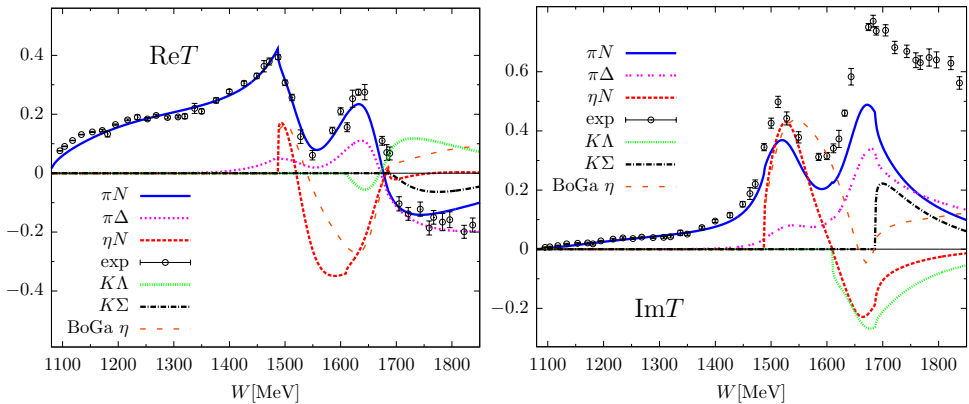


**Fig. 1.** The real and imaginary parts of the scattering T matrix for the dominant  $\pi N$ ,  $\pi\Delta$ ,  $\eta N$ ,  $K\Lambda$  and  $K\Sigma$  channels in the S<sub>11</sub> partial wave. The corresponding thin curve denote the 2014-2 solution of the Bonn-Gatchina group [17] for the  $\eta N$  channel. The data points for the elastic channel are from the SAID partial-wave analysis [18].

present calculation we put the mixing angle  $\theta$  to the popular value of  $30^\circ$  and assume that all meson-quark coupling constants are fixed at their quark-model

values dictated by the SU(3) symmetry. While the real part of the elastic amplitude is well reproduced, the imaginary part is rather strongly underestimated in the region of the second resonance which can be to some extent attributed to too strong couplings in the  $\pi\Delta$ ,  $K\Lambda$  and  $K\Sigma$  channels. This discrepancy should be taken into account when assessing the quality of the photoproduction amplitudes in the following.

### 3 The $\eta$ photoproduction amplitudes

The electromagnetic amplitude in (1) in the S11 partial wave is dominated by the photon-quark coupling while the coupling to the pion cloud turns out to be small. The spin doublet and quadruplet states involve quarks excited to the p orbit with either  $j = \frac{1}{2}$  or  $j = \frac{3}{2}$  [19]:

$$|{}^4\mathbf{8}_{\frac{1}{2}}\rangle = \frac{1}{3} |(1s)^2(1p_{3/2})^1\rangle + \frac{\sqrt{8}}{3} |(1s)^2(1p_{1/2})^1\rangle, \quad (2)$$

$$|{}^2\mathbf{8}_{\frac{1}{2}}\rangle = -\frac{2}{3} |(1s)^2(1p_{3/2})^1\rangle + \frac{\sqrt{2}}{6} |(1s)^2(1p_{1/2})^1\rangle + \frac{\sqrt{2}}{2} |(1s)^2(1p_{1/2})^1\rangle', \quad (3)$$

where the last two components with  $p_{1/2}$  correspond to coupling the two s-quarks to spin 1 and 0, respectively; the flavour (isospin) part is not written explicitly. The quark part of the dominant  $E_{0+}$  transition operator can be cast in the form

$$\int d\mathbf{r} \mathbf{j}^q \cdot \mathbf{A}_{11}^e = i \sum_{i=1}^3 \left[ \mathcal{M}_{\frac{1}{2}} \Sigma_{11}^{[\frac{1}{2} \frac{1}{2}]}(i) + \mathcal{M}_{\frac{3}{2}} \Sigma_{11}^{[\frac{3}{2} \frac{1}{2}]}(i) \right] \left[ \frac{1}{6} + \frac{1}{2} \tau_0(i) \right], \quad (4)$$

where

$$\mathcal{M}_{\frac{1}{2}} = \sqrt{\frac{2}{3}} \int d\mathbf{r} r^2 \left[ j_0(qr) \left( 3v_{\frac{1}{2}}^p(r) u^s(r) + u_{\frac{1}{2}}^p(r) v^s(r) \right) - 2j_2(qr) u_{\frac{1}{2}}^p(r) v^s(r) \right], \quad (5)$$

$$\mathcal{M}_{\frac{3}{2}} = \sqrt{\frac{2}{3}} \int d\mathbf{r} r^2 \left[ 2j_0(qr) u_{\frac{3}{2}}^p(r) v^s(r) + \frac{1}{2} j_2(qr) \left( u_{\frac{3}{2}}^p(r) v^s(r) - 3v_{\frac{3}{2}}^p(r) u^s(r) \right) \right]. \quad (6)$$

The quark transition operator is defined through  $\langle l j m_j | \Sigma_{LM}^{[j \frac{1}{2}]} | \frac{1}{2} m_s \rangle = C_{\frac{1}{2} m_s LM}^{j m_j}$ .

Evaluating (4) between the resonant states and the nucleon we notice that for the proton, the isoscalar part of the charge operator exactly cancels the isovector part in the case of the first two components in (2) and (3). This is a general property known as the Moorhouse selection rule [20] and follows from the fact that the flavour part in these two components corresponds to the mixed symmetric state  $\phi_{M,S}$ . The proton therefore receives no contribution from the  $1s \rightarrow 1p_{3/2}$  transition. This is not the case with the neutron which receives contributions from all components in (2) and (3). The quark in the  $1p_{3/2}$  orbit has a distinctly different radial behaviour from that in the  $1p_{1/2}$  orbit, which is reflected in a different  $q$ - and  $W$ -behaviour of the amplitudes (5) and (6).

The  $E_{0+}$  amplitudes are shown in Fig. 2 for the proton and the neutron in the region of the  $K\Sigma$  threshold. Our results do show a (bump-like) structure in the  $\gamma n$

channel, which is absent in the  $\gamma p$  channel, though its strength in the imaginary part is lower compared to the Bonn-Gatchina 2014-2 analysis (which fits well the experimental cross-section). A moderate rise of the neutron real amplitude below the  $K\Sigma$  threshold is clearly a consequence of the contribution from the  $j = 3/2$  orbit, while the cusp-like drop in the amplitudes is due to the  $K\Sigma$  threshold. This

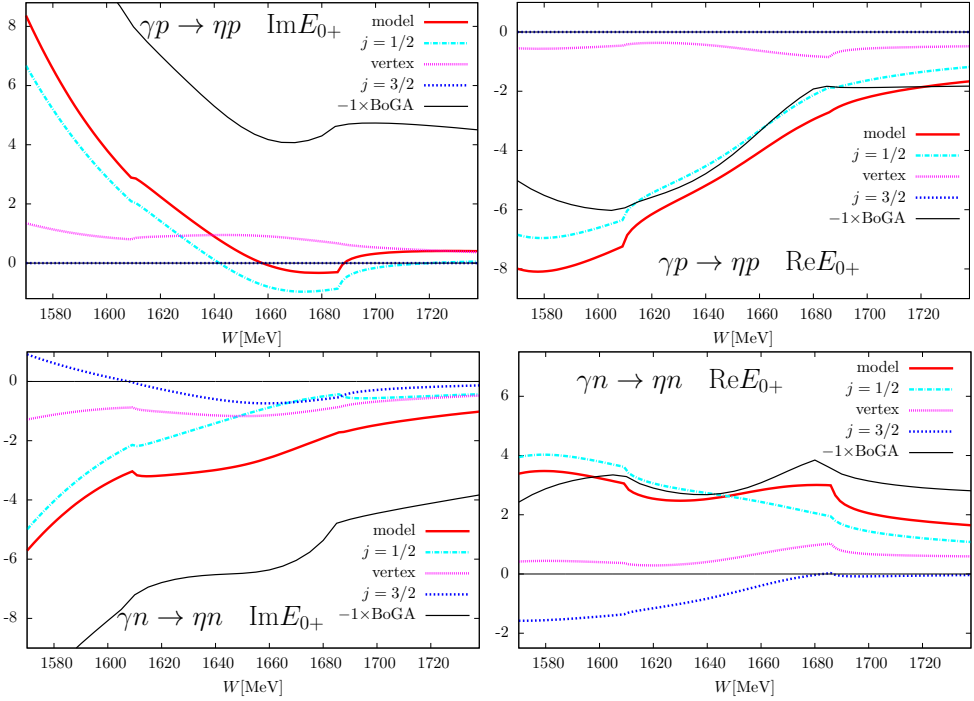


**Fig. 2.** The dominant contributions to the imaginary and real part of the  $E_{0+}$  amplitude (in units of mfm) for the proton (upper two panels) and for the neutron (lower two panels). Apart of the separate contributions from the  $s \rightarrow p_{3/2}$  and  $s \rightarrow p_{1/2}$  transitions the vertex correction is also displayed. The Bonn-Gatchina results are taken from the 2014-2 dataset and multiplied by  $-1$ .

behaviour of the amplitudes is reflected in the cross-section as a peak (bump) present only in the neutron channel (see Fig. 3). Though the strength in our model is lower compared to the Bonn-Gatchina analysis, the qualitative agreement does offer a possible and straightforward explanation of this structure in terms of the quark model: a combination of a peculiar property of the (relativistic) wave functions of the  $S_{11}$  resonances and the presence of the  $K\Sigma$  threshold. Let us stress that the proposed explanation of the considered peak would not be possible in a framework of the nonrelativistic quark model in which the radial behaviour of the quark wave function depends only on the orbital momentum quantum number.

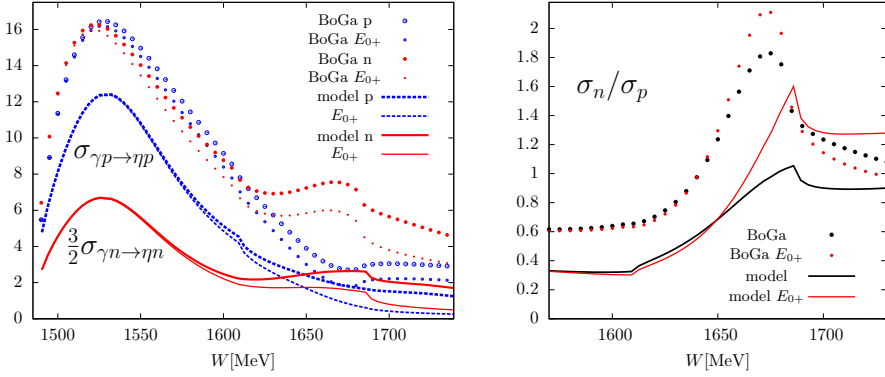


**Fig. 3.** The total cross-sections for  $\gamma p \rightarrow \eta p$  and  $\gamma n \rightarrow \eta n$  (multiplied by the conventional factor of  $\frac{3}{2}$ ) (right panel), the ratio of the neutron and the proton cross-section (left panel). Thinner circles and lines: contribution of the  $S_{11}$  partial wave. The BoGa curves have been reconstructed from the Bonn-Gatchina 2014-2 data set [17].

## 4 Relation to the Single Quark Transition Model

Our model can be envisioned as a version of the Single Quark Transition Model (SQTm) in which the photon interacts with a single quark in the three-quark core and the other two quarks act as spectators. The general form of the SQTm operator is a product of the boost operator and current operators [21]:

$$B_j^\lambda = \sum_{lSL} M_{lSL}^\lambda \mathcal{T}(l, S, L, \lambda) = \sum_{l_z S} R_{l_z S}^\lambda \mathcal{T}(l, l_z, S, S_z = \lambda - l_z), \quad (7)$$

where

$$M_{lSL}^\lambda = C_{l_z S \lambda - l_z}^{L\lambda} R_{l_z S}^\lambda, \quad \langle l || T || 0 \rangle = 1 \quad \text{and} \quad \langle \frac{1}{2} || T(S) || \frac{1}{2} \rangle = \sqrt{2S+1}.$$

In our approach the quark states are labeled by the total angular momentum  $j$ ,  $j_z$  rather than the orbital angular momentum and spin. In this case it is more convenient to expand (7) as

$$B_j^\lambda = \sum_{j_l L} \mathcal{M}_{j_l L}^\lambda \Sigma_{L\lambda}^{[j \frac{1}{2}]}, \quad \langle j || \Sigma_L^{[j \frac{1}{2}]} || 0 \frac{1}{2} \rangle = \delta_{j, l \pm \frac{1}{2}}.$$

Recoupling the angular momenta we find

$$\begin{aligned} \mathcal{M}_{j_l L}^\lambda &= \sum_{S=0,1} (-1)^{j+L-S-\frac{1}{2}} \sqrt{2(2L+1)(2S+1)} W(j_l S \frac{1}{2}; \frac{1}{2} L) M_{lSL}^\lambda \\ &= (-1)^{j+L-\frac{1}{2}} M_{l0l}^\lambda + (-1)^{j+L+\frac{1}{2}} \sqrt{6(2L+1)} W(j_l 1 \frac{1}{2}; \frac{1}{2} L) M_{l1L}^\lambda, \end{aligned}$$

where  $W$  are the Racah coefficients.

In the case of  $S_{11}$  resonances  $l = 1$ , and only the  $E1$  multipole is involved ( $L = 1, \lambda = 1$ ). In this case the coefficients (5) and (6) read

$$\begin{aligned} \mathcal{M}_{\frac{1}{2}} &= \mathcal{M}_{1 \frac{1}{2} 1} = -M_{101}^1 + \sqrt{2} M_{111}^1 = -e_1^{11} + \sqrt{2} m_1^{11}, \\ \mathcal{M}_{\frac{3}{2}} &= \mathcal{M}_{1 \frac{3}{2} 1} = M_{101}^1 + \frac{1}{\sqrt{2}} M_{111}^1 = e_1^{11} + \frac{1}{\sqrt{2}} m_1^{11}, \end{aligned}$$

where  $e_1^{11}$  and  $m_1^{11}$  are the "quark electric" and "quark magnetic" multipole moments. Table 1. in [21] gives for the corresponding E1 baryon multipole moment of the proton and the neutron which in turn can be related to (5) and (6):

$$\begin{aligned} {}_p E1 &= \sqrt{\frac{1}{3}} e_1^{11} - \sqrt{\frac{2}{3}} m_1^{11} = -\frac{1}{\sqrt{3}} \mathcal{M}_{\frac{1}{2}}, \\ {}_n E1 &= -\sqrt{\frac{1}{3}} e_1^{11} + \sqrt{\frac{2}{27}} m_1^{11} = \frac{1}{9\sqrt{3}} \left[ 5\mathcal{M}_{\frac{1}{2}} - 4\mathcal{M}_{\frac{3}{2}} \right], \end{aligned}$$

in agreement with our conclusion that the  $j = \frac{3}{2}$  orbit contributes only in the  $\gamma n \rightarrow \eta n$  channel, which explains the different behaviour of the  $\eta p$  and  $\eta n$  channels in  $\eta$  photoproduction.

## References

1. V. Kuznetsov *et al.*, Phys. Lett. B **647**, 23 (2007).
2. Ya. Azimov *et al.* Eur. Phys. J. A **25**, 325 (2005).
3. M. Döring, K. Nakayama, Phys. Lett. B **683**, 145 (2010).
4. R. Shyam and O. Scholten, Phys. Rev. C **78**, 065201 (2008).
5. V. Shklyar, H. Lenske, U. Mosel, Phys. Lett. B **650**, 172 (2007).
6. V. Shklyar, H. Lenske, U. Mosel, Phys. Rev. C **87**, 015201 (2013).
7. A. V. Anisovich *et al.*, Eur. Phys. J. A **41**, 13 (2009).
8. A. V. Anisovich *et al.*, Eur. Phys. J. A **51**, 72 (2015).
9. X.-H. Zhong, Q. Zhao, Phys. Rev. C **84**, 045207 (2011).
10. B. Golli, S. Širca, Eur. Phys. J. A **52**, 279 (2016).
11. E. A. Veit, B. K. Jennings, A. W. Thomas, R. C. Barret, Phys. Rev. D **31**, 1033 (1985).
12. P. Alberto, L. Amoreira, M. Fiolhais, B. Golli, and S. Širca, Eur. Phys. J. A **26**, 99 (2005).
13. B. Golli and S. Širca, Eur. Phys. J. A **38**, 271 (2008).
14. B. Golli, S. Širca, and M. Fiolhais, Eur. Phys. J. A **42**, 185 (2009).
15. B. Golli, S. Širca, Eur. Phys. J. A **47**, 61 (2011).
16. B. Golli, S. Širca, Eur. Phys. J. A **49**, 111 (2013). Eur. Phys. J. A **49**, 111 (2013).
17. <http://pwa.hiskp.uni-bonn.de/>.
18. [http://gwdac.phys.gwu.edu/analysis/pr\\_analysis.html](http://gwdac.phys.gwu.edu/analysis/pr_analysis.html).
19. F. Myhrer and J. Wroldsen, Z. Phys. C **25**, 281 (1984).
20. R. G. Moorhouse, Phys. Rev. Lett. **16** 772 (1996).
21. W.N. Cottingham and L.H. Dunbar, Z. Physik C **2**, 41 (1979).